Sharif University of Technology

Scientia Iranica

Transactions on Mechanical Engineering

https://scientiairanica.sharif.edu

The variations of breakup and non-breakup regions for ferrofluid microdroplets in T-junctions with a proposed correlation

Mohammad Aboutalebi [a], Omid Adibi [b], Mohamad Ali Bijarchi [a], Mohammad Behshad Shafii [a,*], Siamak Kazemzadeh Hannani [a]

a. Department of Mechanical Engineering, Sharif University of Technology, P. O. BOX: 11155_9567, Tehran, Iran.
b. Energy and Environment Research Center, Energy Management Group, Niroo Research Institute, Tehran, Iran.

* Corresponding author: behshad@sharif.edu (M.B. Shafii)

Received 20 November 2020; received in revised form 30 December 2023; accepted 31 July 2024

Keywords

Ferrofluid;
Magnetic field;
Microdroplets;
Breakup;
Non-breakup;
T-junction.

Abstract

Lots of attention has been paid to microfluidic and nanofluidic instruments in recent decades. One of the interesting instruments in this field that has attracted scientists is T-junctions. This paper reports an empirical study on the variation of breakup and non-breakup regions for ferrofluid microdroplets in symmetrical T-junctions under an asymmetrical magnetic field in the center of the junction. The asymmetrical magnetic field was generated using a permanent magnet on the right side of the T-junction. During the tests, ferrofluid microdroplets with different lengths and various velocities were entered into the T-junction and were influenced by an asymmetrical magnetic field. Results show that the increment in the magnetic flux density causes a higher possibility of non-breakup for ferrofluid microdroplets. Therefore, the breakup and non-breakup region in the diagram of non-dimensional length versus *Ca* number shifts upward. On the other hand, it was observed that the increment in *Ca* number is a key factor in breaking the microdroplets in the T-junction. Finally, a correlation was proposed to predict the breakup and non-breakup region due to different amounts of magnetic flux density and *Ca* number.

1. Introduction

Since lots of attention has been focused on microfluidic instruments in recent years, the use of these devices has been greatly expanded in academic and industrial fields [1-3]. The concept of droplet microfluidics involves the controlled production and manipulation of nano- to femtolitre droplets of a fluid phase in another fluid that is immiscible with the first [4]. The interesting features of microfluidic instruments, such as controllability, safety, and negligible cost, have trusted scientists to use them in different fields [5,6]. They can be used in different applications such as catalyst reactions, separation procedures, micropumps, biologic analyses, and so on [7-10]. In recent years, there has been a lot of research that has been done on single-cell omics applications of microfluidics, such as the study of sperm-surface interactions [11,12]. A high-throughput drug screening method using droplet microfluidics is another application being investigated by researchers. They study how drugs could be properly delivered to relevant organs using microfluidic concepts [13,14]. In tissue and protein engineering, this concept could also be used to analyze their structures better [4,15]. Its wide range of applications has made microfluidics an interesting and challenging topic for researchers across a variety of sectors.

Symmetrical T-junctions are one of the most interesting topics in microfluidics [16,17]. They are commonly applied to make breaks in microdroplets [18-22]. In this method, a microdroplet moves toward a T-junction with the continuous flow. This microdroplet is known as the mother microdroplet. As the mother microdroplet arrives at the T-junction, it can be broken into smaller droplets dependent on the surface tension and shear forces [18-25]. Leshansky and Pismen [18] showed numerically that microdroplets within a T-junction could be broken under specific conditions. They obtained the minimum length of microdroplets for certain breakups inside the T-junction as a function of the microdroplet velocity inside the microchannel and proposed

To cite this article:
M. Aboutalebi, O. Adibi, M.A. Bijarchi, M.B. Shafii, S. Kazemzadeh Hannani "The variations of breakup and non-breakup regions for ferrofluid microdroplets in T-junctions with a proposed correlation", Scientia Iranica (2025) **32**(2): 5113 https://doi.org/10.24200/sci.2024.57207.5113.

an analytical relation that depicted the border curve between breakup and non-breakup regions. Also this year, Jullien et al. [22] experimentally investigated the phenomenon of microdroplet breakup in low capillary numbers within symmetrical T-junctions and observed that two certain flow regimes of "breakup" and "non-breakup" occur in them. In 2019, Jangir and Jana [25] investigated the process of droplet breakup in a 3-D model, using a conservative Level Set method. They observed that the new model has good agreement with previous ones, and the results are similar to other investigations in this field. In all of the mentioned cases [18-25], it is clear that if the T-junction is completely symmetrical (the width and length of the branches and internal thickness of each branch, and so on are perfectly similar), and the microdroplet breaks, each branch will receive exactly half of the volume of the mother microdroplet. In this case, the splitting ratio is 0.5, which depicts symmetric splitting [26]. Also, if the microdroplet inside the symmetrical T-junction does not split, the splitting ratio will be 1 [26].

Typical T-junctions can only produce a breakup ratio of 0.5 or 1 [26]. Actually, because of the existence of symmetry in the T-junction, the breakup ratio can only be 1 or 0.5. Contrarily, it is occasionally required to put more control over the behavior of the microdroplets in the T-junctions to achieve other amounts for splitting ratio [19,20,26,27]. For this purpose, it is necessary to make some changes in the geometry of the T-junction or put an asymmetry in the initial conditions of the issue. Therefore, to alter the geometrical specifications, the width or the length of the microchannel branches can be changed. Since these variations, the mother microdroplet gets asymmetric breakup. In fact, hydrodynamic resistances of the connecting branches are changed due to the variations in the geometry [19,20,24,26,27]. Bedram and Moosavi [20] depicted that if the lengths of the branches are different, a smaller amount of the mother microdroplet goes into the longer branch after a breakup. Also in 2013, Salkin et al. [24] described that utilizing obstacles in the microchannel can thrust the microdroplets to an asymmetric breakup. In that year, Samie et al. [27] illustrated experimentally that if the width of the microchannel branches is different from each other, then a larger amount of the mother microdroplet tends to enter the branch that is wider. In 2019, Raveshi et al. [28] studied the asymmetric splitting of droplets in a closed-loop T-junction with a single-layer valve. They reported that the change in the position of the valve can control the splitting ratio. In 2020, Agnihotri et al. [29] examined a closed system of droplet production with two T-junctions and observed different situations of breakup and non-breakup due to different conditions.

Furthermore, using a magnetic field is another method that has been attained in manipulating the breakup process [30-34]. Adding magnetic particles to different fluids can produce magnetic properties, which can be manipulated by a magnetic field [32-36]. This type of fluid is called ferrofluid. Ferrofluids have been used in different fields, such as droplet formation [37-41], droplet [42,43] and marble [44,45] manipulation, and heat transfer enhancement [46]. One of the methods that can cause asymmetrical splitting in T-junctions is the presence of an asymmetric magnetic field in the center of the joint [26,47-49]. In 2018, Aboutalebi et al. [26] conducted a symmetrical T-junction with asymmetrical magnetic. They depicted that, in this case, there will be more control over the breakup phenomenon. The ferrofluid microdroplets can be influenced by the magnetic force and split into two daughter droplets with different volumes. Also, they described an analytical equation, which was a function of *Ca* and Magnetic Bond number, to predict the border curve of breakup and non-breakup numerically. In another work, Aboutalebi et al. [48] studied the effect of an asymmetrical magnetic field on the performance of asymmetrical T-junctions numerically. They reported that the combination of the asymmetrical magnetic field with variations in the width ratio of T-junction's branches can help to reach a wide range of splitting ratios.

Hence, breakup ratio, *BR*, or splitting ratio can be defined as "the volume of the microdroplet enters to the branch with less hydrodynamic resistance divided to the total volume of the mother microdroplet" [26,48]. $BR = 1$ means non-breakup, and $BR = 0.5$ reflects symmetric breakup. In this case, it is probable to achieve a splitting ratio between 0.5 to 1 [26,48].

In previous investigations, utilizing magnetic force to study the phenomenon of microdroplet breakup is conducted [47,48,50,51]. However, the variations of the border curve between the breakup and non-breakup regions and describing an analytical equation for them to predict it for different amounts of *Ca* numbers have not been investigated empirically in T-junctions. The purpose of this paper is to study the prominent factors on the variation of the border curve of breakup and non-breakup and achieve an empirical relation to predicting this border for different values of *Ca* numbers, non-dimensional length, and magnetic flux density.

2. Materials and methods

2.1. Physics of the problem

To study the phenomenon of ferrofluid microdroplet breakup in T-junctions, it is necessary to introduce the physics of the issue. The forces exerted on the ferrofluid microdroplets at the T-junction in the presence of a magnetic field can be explained as three main forces [19,20,26,27].The first one is "Inertial force". This force acts on the back of the microdroplet due to the continuous fluid motion. Olive oil is used as the continuous fluid in this investigation. The other force which exists is "Surface tension". This force affects the microdroplet in motion and prevents it from breaking up. The last force is the "Magnetic force" resulting from the magnetic field. In addition to the previous forces which affect the moving ferrofluid microdroplets, an external body force resulting from the magnetic field is also exerted on the microdroplet. The existence of this magnet at different distances from the origin causes different volumetric forces to be exerted on the microdroplet. As a result, this force must be related to the magnetic field, $\vec{M}$, and the gradient of magnetic field strength, $\vec{H}$. The following equation is proposed to calculate the external magnetic force on the ferrofluid microdroplets:

$$\vec{f} = \mu_0 \vec{M} \nabla \vec{H}, \quad (1)$$

where the magnetic field strength $\vec{H}$ has the unit of A/m, and μ_0 is the free space permeability and equals $4\pi \times 10^{-7}$ N/A^2. For low temperatures and a limited range of magnetic fields, the magnetization field $\vec{M}$ can be written as a function of magnetic field intensity $\vec{H}$ [7]:

$$\vec{M} = \chi_m \vec{H}, \quad (2)$$

which χ_m is magnetic permeability.

2.2. Materials

To generate and study the ferrofluid microdroplet behavior in T-junctions, two fluids are required as continuous and discrete phases. For the experiments, the required ferrofluid synthesized in the laboratory was water-based ferrofluid. The ferrofluid microdroplets as discrete fluids were generated from this water-based fluid. Also, olive oil was selected as the continuous phase.

In order to make the ferrofluid which was used in the experiments to produce mother microdroplets as a discrete phase, the following stages were implemented: First, deoxygenated distilled water was poured into an Erlenmeyer flask, and in order to extract all the oxygen in the container throughout the ferrofluid preparation, nitrogen gas was blown into the system. Next, 10.812 g of ferric chloride (6.H_2O) with a molar mass of 270.295 g/mol and 3.976 g of ferrous chloride (4.H_2O) with a molar mass of 81.198 g/mol were added to the distilled water.

In this stage, the solution in the Erlenmeyer flask was stirred at 1000 rpm on a hotplate stirrer. In this stage, the temperature is raised to 70°C and after the complete solution of salts was ensured, 50 ml of ammonium hydroxide was added dropwise to the solution with a burette. The addition of ammonium hydroxide continued until the pH of the solution reached 10. This process slightly turned the color of the solution from brown to black, which indicated the formation of magnetite particles. In this state, the temperature was increased to 80°C, held for an hour, and then magnetite nanoparticles were washed. For washing and separation of excess ammoniac and other impurities, deoxygenated distilled water was used. Additionally, the strong magnetic field of a magnet was used to separate the liquid from the nanoparticles. This magnetic field absorbed the nanoparticles. After the separation of nanoparticles, distilled water was added to them and the resulting solution was stirred to remove the residual ammonia, and separation was again performed by the strong magnet. This procedure was repeated 3 to 5 times until the pH reached 7. Surfactant, as a chemical compound that reduces surface tension and interfacial tension, was added to the resulting moist powder, mixed with the stirrer, and eventually, 100 ml distilled water was added, and the solution was put inside a sonicator device for 10 minutes. This method was used to produce water-based ferrofluid as a dispersed phase for the ex periments. The ferrofluid as the discrete phase has ρ_d=1050 kg/m^3 and μ_d=2.11 mPa.s. The resulting fluid was stimulated in response to the magnetic field, and the intensity of stimulation was directly proportional to the intensity of the magnetic field. The magnetization curve for the ferrofluid

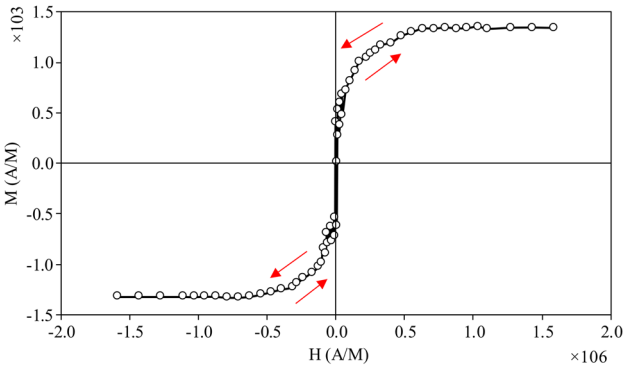

Figure 1. Magnetization curves of the ferrofluid that is used in the present study.

Table 1. The properties of fluids.

Materials	Density (kg/m^3)	Dynamic viscosity (mPa.s)
Olive oil	912	99.5
Ferrofluid	1050	2.11

that is used in the present study is provided in Figure 1. It shows that the effect of the magnetic field on the magnetization of the ferrofluid is quite sensitive as long as it is below the saturation point, even if a considerably small magnetic field is applied.

Olive oil was selected as a continuous phase with the density and viscosity of ρ_c=912 kg/m^3 and μ_c=99.5 mPa.s, respectively. Also, the surface tension between oil and ferrofluid was measured to be σ=2.8 mN/m. Calculation of this value was based on separate experiments using tensiometer. This value is supposed to be constant during the experiments. The properties of fluids used in the paper are listed in Table 1. The properties of continuous and discrete phases are assumed to be constant during all the experiments.

Metallic nanoparticles with magnetic properties (iron, nickel, cobalt, and so on.) are suspended in a liquid consisting of a nanofluid with a particle size of 10-100 nm. Initially, nanoparticles are homogeneously dispersed in liquids because of their small size. As particles join to each other over time, their colloidal properties are lost, the particles settle in the solution, and the magnetic properties of the solution are lost as well. One side of these surfactant particles connects to the colloid, and the other side connects to the solution. Hence, the heads that have the same name cause repulsion between colloids and prevent particles from joining together, thereby maintaining the magnetic properties of solutions. Following the above-mentioned method, nanoparticles with an average diameter of 50 nm were produced in this study.

2.3. Experimental setup

The goal of this study was to investigate the effect of a permanent magnet and its magnetic flux density on the ferrofluid mother microdroplet breakup in a T-junction. The schematic of the utilized T-junction in the experiments can be seen in Figure 2.

To fabricate a suitable microchannel for running the experiments, these steps have been taken: first, the mold of the microchannel was produced using the 3-D print method. The Poly Di Methyl Siloxane (PDMS) elastomer and curing agent were mixed with a ratio of 10 to 1 and placed in a vacuum chamber until the mixture was completely degassed.

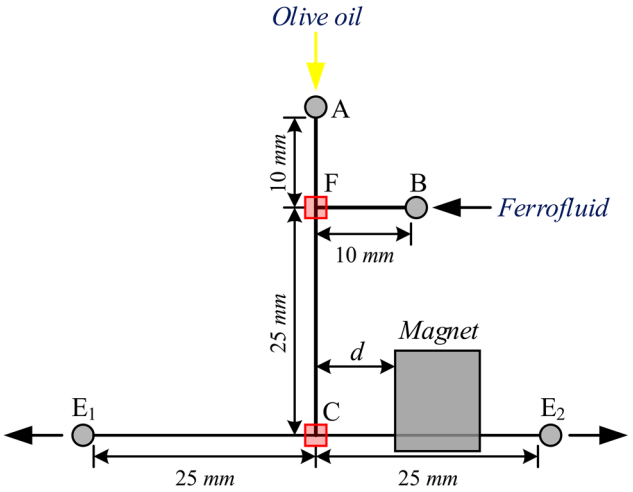

Figure 2. The schematic and dimensions of the microchannel. The width and depth of all the branches are 400 and 200 µm, respectively.

A PDMS layer was covered on the mold and was baked for 20 minutes in the oven. The temperature of the oven was 170°C. Then, the produced layer was cut off from the mold and bonded on a glass slide. The thickness of the coated PDMS layer and glass slide were 4 and 1 mm, respectively. Also, the width and the depth of the microchannel branches were 400 and 200 µm, respectively. The accuracy of microchannel manufacturing is less than 1%. Then, the width and depth of the microchannel used in this research were assumed constant in any section of the microchannel.

Figure 3 shows the experimental setup used in this study. Olive oil as the continuous phase and the ferrofluid as the discrete phase enter the main and side channels via indicated tubing connectors (point *A* and point *B* in Figure 2, respectively). Two syringe pumps (FNM, SP1000HPM) were used to transfer both fluids into the microchannel. The accuracy of each syringe pump was 0.001 ml/h.

As the ferrofluid approaches the oil inside the main microchannel (point *F* in Figure 2), ferrofluid microdroplets are formed and move towards the center of the T-junction (point *C* in Figure 2). To record the movement of microdroplets inside the T-junction, a high frame rate camera (Nikon 1 J4) with 1200 fps was used, and a small LED lamp was placed below the microchannel to improve the quality of images. Finally, a magnet was placed at a distance of *d* from the T-junction (as seen in Figure 2), and the behavior of microdroplets at the T-junction was recorded by the camera.

The data on the camera were examined with a customized image processing software, DMV [52]. This software is a powerful tool for determining the length and velocity of microdroplets and the volume of mother and daughter microdroplets. The length of the mother microdroplet (L) was measured with this software and was non-dimensionalized using the width of the microchannel (W) as L/W. Capillary number, which is the ratio of continuous fluid's inertial force to the surface tension force, is defined as $Ca = \frac{\mu_c u}{\sigma}$ in which u indicates the mean velocity of the continuous phase. The Ca is determined in the main channel, which connects to the T-junction. In fact, this parameter is for microdroplets after their formation (point F) in the main channel till they arrive at the center of the T-junction (Point C). Also, μ_c denotes the dynamic viscosity of the continuous phase (olive oil), and σ is the surface tension.

As can be seen in Figure 2, a permanent magnet (Neodymium magnet with the size of 20 mm × 10 mm × 5 mm) was placed at a distance of d from the center of the T-junction on the right branch to produce a magnetic field. The magnitude of the magnetic flux density at the center of the T-junction could be changed just by altering the distance d. To determine the variation of the magnetic flux density of the permanent magnet with the distance from the center of the magnet, a gauss meter with an accuracy of 0.01 mT (Lutron MG-3003SD) was used. According to Figure 4, to determine the magnetic flux density, the probe of the gauss meter was placed at different distances from the middle part of the left side of the magnet. Figure 4 shows the variation of magnetic flux density with distance from the edge of the magnet.

Also, by analysis of camera records, the volume of daughter microdroplets that go to the right side and left side was calculated, and then the breakup ratio was determined. The breakup ratio is defined as the ratio of the volume of the daughter microdroplet which moves into the right branch (which has less resistance due to the existence of the permanent magnet) to the total volume of the ferrofluid mother microdroplet. As was discussed before, there are generally two possibilities for the ferrofluid mother microdroplet when it reaches the T-junction in the absence of a magnetic field. It might exit through one of the branches without splitting, or it can be divided into two daughter microdroplets with equal volumes, each exiting through a separate branch. In the latter, since the volumes of the two daughter droplets are identical, the splitting ratio becomes

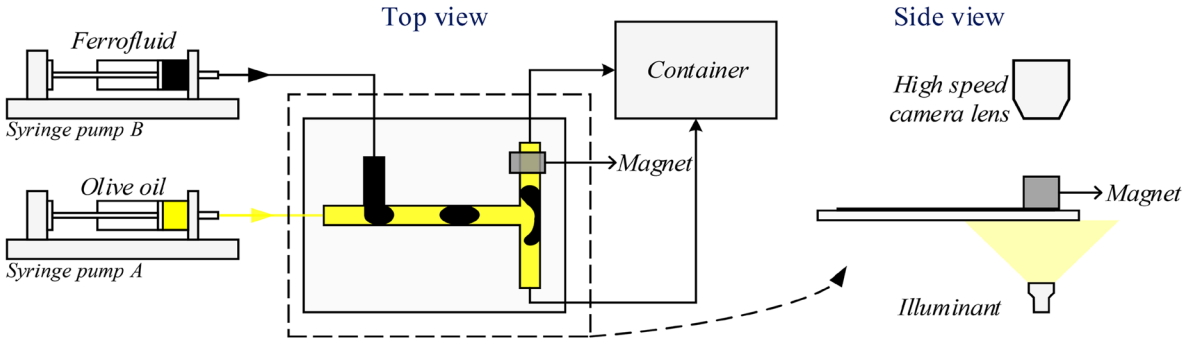

Figure 3. The schematic of the experimental setup

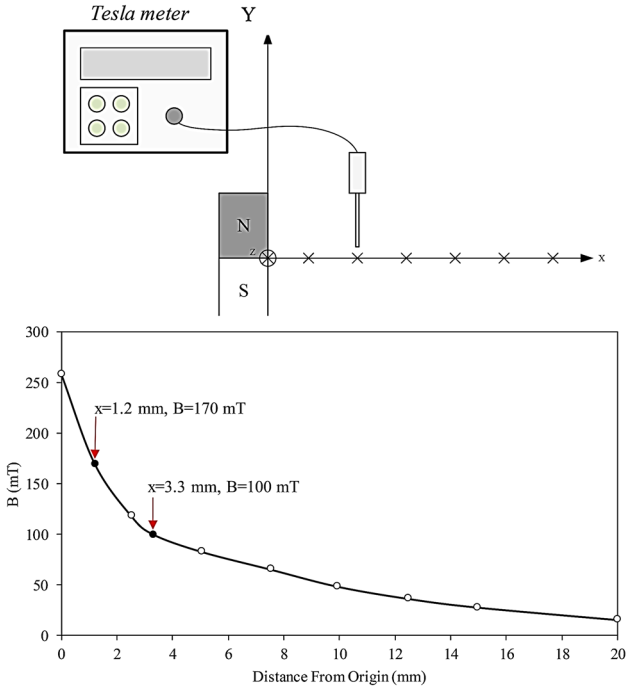

Figure 4. The variation of the magnetic flux density of the permanent magnet with the distance from the center of the magnet.

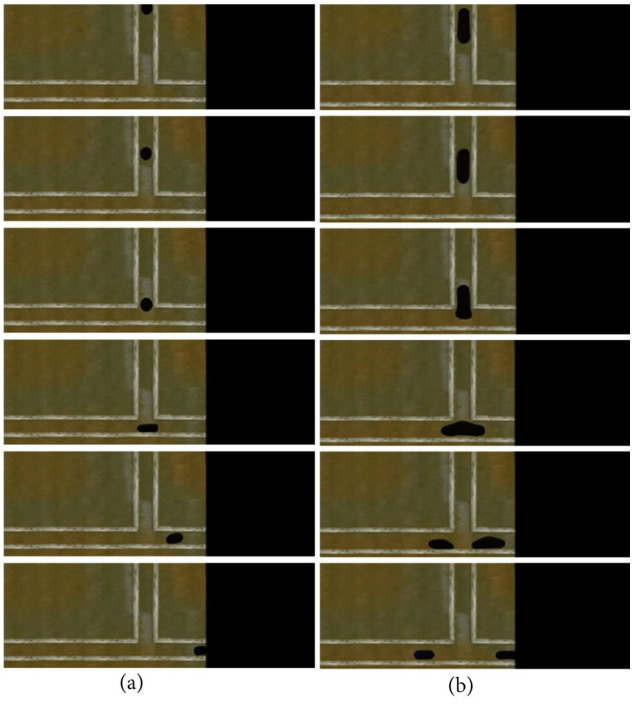

Figure 5. Two ferrofluid microdroplets in T-junction with different regimes of non-breakup and breakup in the presence of a permanent magnet (a) L/W = 1.05 and BR = 1, (b) L/W = 2.1 and BR =0.622.

0.5 due to Eq. (1). According to this definition, a breakup ratio of 0.5 indicates a symmetrical breakup of the microdroplet, and a breakup ratio of 1 means the mother microdroplet has not broken up. However, if a magnet is placed on the right branch of the T-junction, as seen in Figure 5, a larger volume of the microdroplet enters the right branch due to the interaction of the magnet and the iron particles in the ferrofluid. Therefore, there are two possible scenarios. The first scenario can be seen in Figure 5(a), which is that by passing the ferrofluid microdroplet from the T-junction, the whole volume exits from the right branch, which the magnet is placed, and has less resistance in comparison with the left branch. In this case, the breakup ratio becomes 1. The second scenario, as can be observed in Figure 5(b), is that the ferrofluid microdroplet is divided into two daughter microdroplets, but this time not necessarily with a breakup ratio of 0.5. Because in this case, the existence of a magnet on the right branch leads to larger breakup ratios than 0.5 due to its influence on magnetic particles in ferrofluid microdroplets. In Figure 5, two ferrofluid mother microdroplets in T-junction with different regimes of breakup and non-breakup in the presence of a permanent magnet are observed. For both cases, u_c=3.02 mm/s (Ca=0.107), $|\vec{B}| = 170$ mT, and the time consequence is 250 ms.

2.4. Methods

The experiments were conducted, and the results were recorded as follows: According to Figure 3, the syringe that was connected to the main channel (syringe A) was filled with olive oil, and the one connected to the right side of the main channel (syringe B) was filled with ferrofluid. Next, the flow rate of syringe A was varied from 0.3 to 15 ml/hr. Then, for each flow rate that was fixed in syringe A, the flow rate in syringe B was varied from 5 to 200% of the flow rate in syringe A. In this way, ferrofluid mother microdroplets were generated in point F in Figure 2. The size of ferrofluid microdroplets was a function of Q_d/Q_c, where Q_d and Q_c denote the flow rate of the continuous phase and disperse phase, respectively. Also, the velocity of ferrofluid microdroplets had a unique relationship with the flow rate of syringe A. Hence, these ferrofluid microdroplets were moved forward to the center of the T-junction (point C in Figure 2) with a specific velocity and dimensionless length.

3. Validation

To evaluate the correctness of the results obtained from experiments, they should have been verified. The results of microdroplet breakup in our study are validated with the results of Leshansky and Pismen [18].

It is necessary to introduce the concept of two parameters of L and L_c to validate the results. L is the initial length of the mother microdroplet at the start of the process, while the critical length L_c depicts the maximum length of the mother droplet prior to its breakup in the T-junction [18].

Leshansky and Pismen described an analytical equation that can obtain a border between non-breakup and breakup regions. The recommended equation is a function of Ca number and can be defined as [12]:

$$\frac{L_c}{W} = 1.3Ca^{-0.21}, \quad (3)$$

where W is the width of the microchannel. To verify the accuracy of the obtained results, the breakup or non-breakup status of different microdroplets in various Ca numbers in the T-junction without a magnetic field was plotted. These statuses were compared with the analytical equation of Leshansky and Pismen, as can be seen in Figure 6.

Based on Figure 6, it is observed that the present results precisely predict the borderline between splitting and non-splitting regions in the T-junction and are in agreement with the results of Leshansky and Pismen [18].

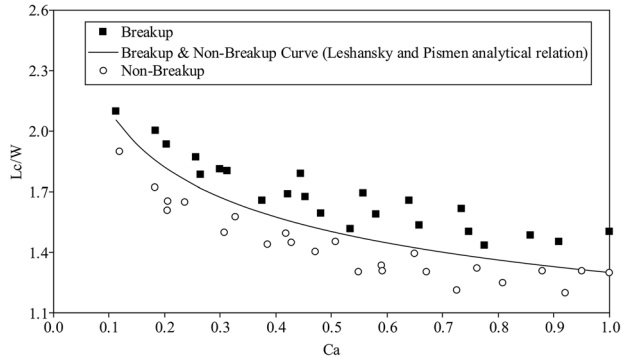

Figure 6. Comparison of results of the current investigation (squares and spot) and the analytical relation of Leshansky and Pismen, which determines the breakup and non-breakup region for a T-junction.

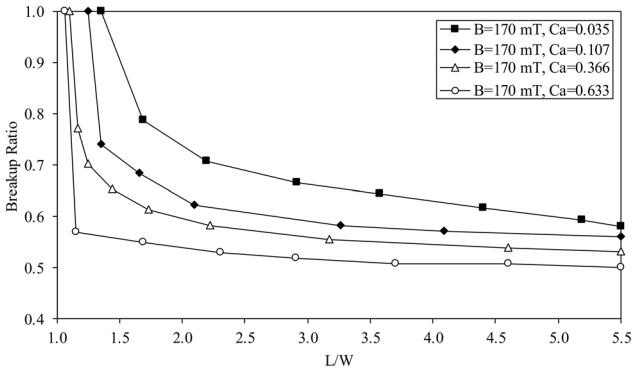

Figure 7. Breakup ratio variations with respect to non-dimensional length for the ferrofluid mother microdroplet in $|\vec{B}|$=170 mT at four different *Ca* numbers.

4. Results

The results of the experiments can be seen in Figures 7 and 8, respectively. Figure 7 shows the variations of the breakup ratio concerning the non-dimensional length of the ferrofluid mother microdroplet for four different *Ca* numbers of 0.035, 0.107, 0.366, and 0.633 in the existence of $|\vec{B}| = 170$ mT. The behavior of the diagram for each *Ca* number is the same. This diagram depicts that as the non-dimensional length of the ferrofluid microdroplet increases in a specific *Ca* number, the breakup ratio gets closer to 0.5, which means a symmetrical breakup. Also, it is shown that for small ferrofluid microdroplets, the breakup ratio is closer to 1 rather than 0.5. More than this, for some non-dimensional lengths of ferrofluid microdroplets, the breakup ratio means that the ferrofluid microdroplet entirely passes through the right branch without breaking. For example, in $|\vec{B}| =$ 170 mT and *Ca*=0.107, for the ferrofluid mother microdroplets whose non-dimensional lengths are smaller than 1.25, the breakup ratio becomes 1. This amount is a critical value for non-dimensional length in the mentioned *Ca* and $|\vec{B}|$. In fact, if the ferrofluid microdroplet, which has a non-dimensional length of less than 1.25, enters the T-junction, it passes through the right branch without breaking due to the smaller resistance of the right branch. In this case, the intensity of the existing magnetic field is strong enough that it can affect the entire volume of the ferrofluid microdroplet and push it into the right branch. As the non-dimensional length increases from 1.25, the breakup ratio reduces asymptotically to reach about 0.5. Generally, at a

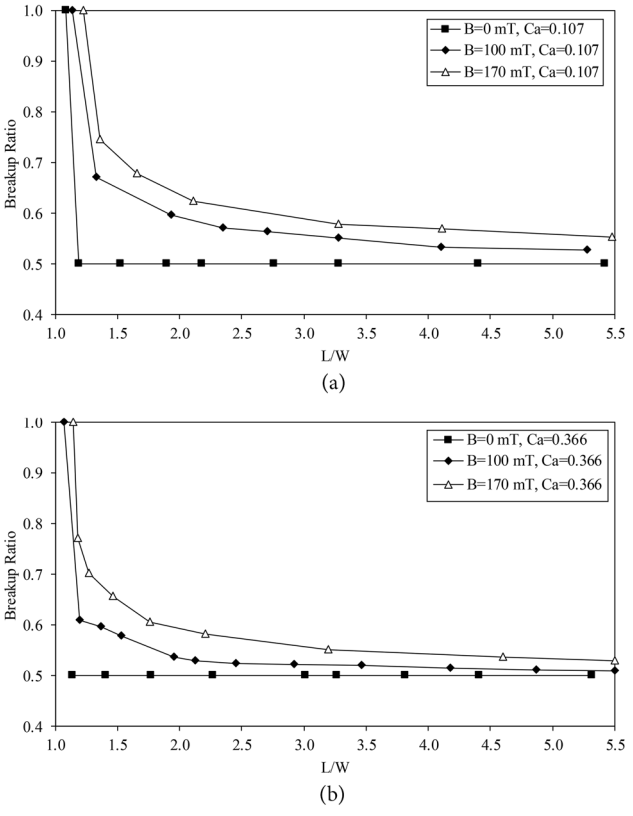

Figure 8. Breakup ratio variations with respect to non-dimensional length for the ferrofluid mother microdroplet at three different values for $|\vec{B}|$ and (a) *Ca* =0.107 and (b) *Ca* =0.366.

constant velocity, as the length of the ferrofluid microdroplets increases, the strength of the fixed magnetic field decreases to influence the whole volume of the ferrofluid mother microdroplet and conduct it to the right branch. The reason for this phenomenon is that as the microdroplet becomes longer, the magnetic field is less likely to pull the entire volume of the mother microdroplet towards itself and only pull a portion of it. Hence, the influence of the magnetic field on the ferrofluid microdroplet breakup decreases. In contrast, when the microdroplet is small, the field is strong enough to pull the entire mother microdroplet, and hence, the breakup ratio becomes 1.

The other worthy point in Figure 7 is that in a lower *Ca* number, the breakup ratio at a certain non-dimensional length increase. For instance, it is shown that in the non-dimensional length of 5.5, the breakup ratio is 0.509, 0.53, 0.552, and 0.582 for *Ca* numbers of 0.035, 0.107, 0.366, and 0.633, respectively. When the ferrofluid microdroplet enters the T-junction with a high *Ca*, due to the high inertia, the ferrofluid microdroplet is more likely to break up symmetrically. Therefore, the increase in the *Ca*, increases the tendency of the ferrofluid microdroplet to break up symmetrically and reduces the breakup ratio. This is while the increase of the magnetic field increases the tendency of microdroplets to break up asymmetrically and soars the breakup ratio. In fact, an increment in the magnetic flux density and the increase in *Ca* number are two parameters that have opposite effects on the phenomenon of ferrofluid microdroplet breakup.

Figure 8 shows the variations of breakup ratio with respect to the non-dimensional length of the microdroplet at *Ca*=0.107 and 0.366 for three different magnetic flux

densities of 0 (without magnetic field), 100 (medium-intensity magnetic field), and 170 mT (high-intensity magnetic field). It should be noted that the upper range of the magnetic field is selected based on the reproducibility and reliability of the experimental results. In addition, the range selected falls within a common one in related studies. The trends of all three curves are descending. This figure shows that when no magnetic field is applied ($|\vec{B}| = 0$), depending on the size of the ferrofluid mother microdroplets, the microdroplets either exit without breaking up (breakup ratio of 1) or break up symmetrically and exit through separate branches (breakup ratio of 0.5). For instance, in Figure 8(a), when $|\vec{B}| = 0$ for the non-dimensional length of 1.1, the breakup ratio is equal to 1. It is clear that in this case, any microdroplet with a non-dimensional length of less than 1.1, enters the center of the T-junction will not break, and the breakup ratio for it will be equal to 1. However, with a slight increase in the microdroplet length from 1.1, the breakup ratio will be 0.5, which means symmetrical splitting. If there is no magnetic field in the system and the T-junction is perfectly symmetrical, the breakup ratio can only be 1 or 0.5, which indicates non-breakup and a perfectly symmetrical breakup of the microdroplet, respectively. Moreover, it can be seen that the situation varies dramatically due to the existence of magnetic flux density in the system. In Figure 8(a), it is obvious that in the presence of the magnetic flux density, the breakup ratio varies in the range of 0.5 to 1. In this case, ferrofluid mother microdroplets with higher non-dimensional lengths are more likely to have a symmetrical breakup and a breakup ratio closer to 0.5.

For example, at *Ca*=0.107 and $|\vec{B}| = 100$ mT, for a specific mother microdroplet with a non-dimensional length of 1.34 (*L/W* = 1.34), the breakup ratio is 0.669. By increasing the amount of *L/W* to 1.91 and 2.68, the breakup ratio decreases to 0.596 and 0.565, respectively.

The other interesting point about this figure is the effect of magnetic flux density on the breakup ratio. According to Figure 8(a), by increasing the magnetic flux density at the T-junction, the likeliness of the asymmetrical breakup of the microdroplet increases, and higher values of the breakup ratio are achievable. Hence, tuning the breakup ratio and obtaining different microdroplet sizes is possible by changing the magnetic flux density. Finally, these results show that it is possible to fine-tune the breakup ratio and obtain the exact sizes of the daughter microdroplets by changing the magnetic field intensity. In Figure 8(a), for instance, for a specific mother microdroplet with a non-dimensional length of 1.34 (*L/W* = 1.34), the breakup ratio is 0.5 due to $|\vec{B}| = 0$. By increasing the value of $|\vec{B}|$ to 100 and 170 mT, the breakup ratio increases to 0.669 and 0.74, respectively. It means that, by altering the value of $\vec{B}$ from 0 to 170 mT, the breakup ratio was enhanced by 48%.

Figure 9 shows the border curve between breakup and non-breakup regions for different values of *Ca* number and dimensionless length in 3 magnetic flux densities of $|\vec{B}| = 0$, 100, and 170 mT (The distance of center of T-junction from the permanent magnet are set to 1.2 mm and 3.3 mm for $|\vec{B}|$ = 100 and 170 mT, respectively.). To plot these graphs, different ferrofluid microdroplets with different velocities entered the T-junction, and breakup or non-breakup of them have been recorded. As mentioned, there are two possibilities

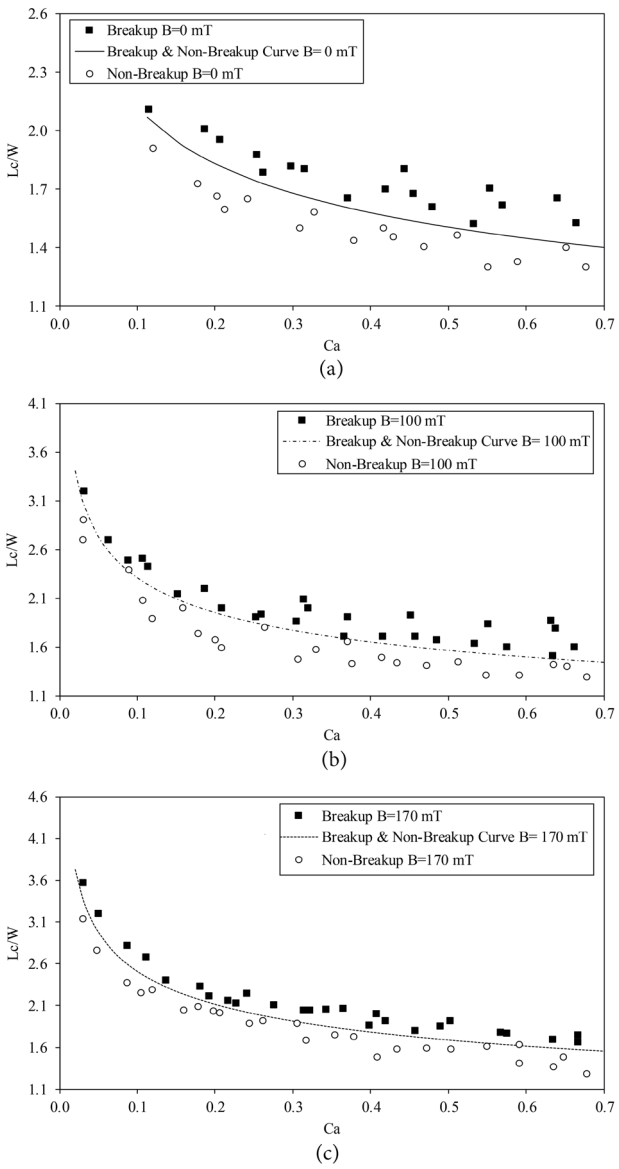

Figure 9. The border curve between breakup and non-breakup regions for three different magnetic flux densities of (a) $|\vec{B}|$ =0 mT, (b) $|\vec{B}|$=100 mT, and (c) $|\vec{B}|$=170 mT. The distance of center of T-junction from the permanent magnet are set to 1.2 and 3.3 mm for $|\vec{B}|$=100 and 170 mT, respectively. The magnetic force is proportional to $B\nabla B$ which is equal to 9420 and 1660 $(mT)^2/m$.

of breakup and non-breakup for ferrofluid microdroplets inserted into the T-junction. It can be seen that in each of these diagrams, the border curve between the splitting and non-splitting zones has a decreasing trend, and with increasing *Ca* number, the minimum critical length of the ferrofluid microdroplets to break up in the junction, decreases. Also, an increment in the non-dimensional length of microdroplets raises the possibility of breakup in the junction. In fact, increasing the *Ca* and non-dimensional length are key factors that help the ferrofluid microdroplets to break at the micro-junction in any amounts of magnetic flux densities.

For a better comparison of breakup and non-breakup border curves, these boundaries are shown in Figure 10. In this graph, it is clear that as the magnetic flux density applied to the center of the T-junction increases, the border curve shifts upward. In other words, by increasing the amount of

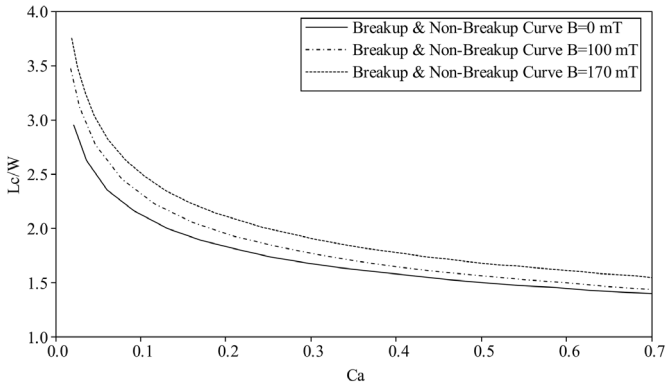

Figure 10. The variations of the border curve due to the existence of magnetic flux density in the diagram of *Ca* with respect to non-dimensional length. The distance of center of T-junction from the permanent magnet are set to 1.2 and 3.3 mm for $|\vec{B}|$=100 and 170 mT, respectively. The magnetic force is proportional to $B\nabla B$ which is equal to 9420 and 1660 $(mT)^2/m$.

$|\vec{B}|$, the non-breakup area expands and progresses to the breakup zone. The magnetic force based on Eq. (1) is proportional to $B\nabla B$. This quantity is calculated based on thevariation of magnetic flux density in Figure 4, and the results show that similar to magnetic flux density $B\nabla B$, decreases as the distance from the magnet increases. Increasing the magnetic force reduces the chance of the ferrofluid microdroplet breaking at the junction. Physically, it can be said that the stronger the magnet in the right branch, the more the total volume of the mother microdroplets will tend to enter the right branch due to less hydrodynamic resistance. Obviously, if the total volume of the microdroplet is not absorbed by the magnet, a percentage of it enters the right branch. Also, if the microdroplet breaks in the junction in the absence of a magnetic field, only half of the mother microdroplet's volume enters the right branch.

As discussed before, Leshansky and Pismen [18] developed an analytical relation to show the border curve between the breakup and non-breakup regions in symmetrical T-junctions. In the current study, a correlation is established to depict the border curve between zones in the presence of the magnetic flux density. It should be noted that all the terms in the proposed correlation must be non-dimensionalized. Hence, it is necessary to put B in a non-dimensional term such as $(\frac{WB^2}{\sigma\mu_0})$ [53-55]. Utilizing the results for different magnetic flux densities and performing curve fitting, the following relation can be obtained as:

$$\frac{L_c}{W} = 1.3Ca^{-0.21} + 0.0003(\frac{WB^2}{\sigma\mu_0})^{0.7456}Ca^{-0.46}. \quad (4)$$

It can be seen that for $|\vec{B}|$=0 mT, Leshansky and Pismen's [18] equation is obtained. In our experiments, the amount of W, σ, and μ_0 were constant parameters. By putting the amounts of these parameters in the equation, it can be simplified to:

$$\frac{L_c}{W} = 1.3Ca^{-0.21} + 37.8B^{1.4912}Ca^{-0.46}. \quad (5)$$

5. Conclusion

In this study, the effect of an asymmetrical magnetic field on the ferrofluid microdroplet breakup phenomenon at a T-junction was investigated. The following results were obtained from the experiments:

- Applying an asymmetrical magnetic field in symmetrical T-junctions can change the amount of breakup ratio as well as the border curve between the breakup and non-breakup region;
- As the *Ca* number of a ferrofluid mother microdroplet inside the main microchannel decreases (the microdroplet velocity decreases), the breakup ratio increases and approaches 1 under a constant asymmetric magnetic field. In fact, decreasing the *Ca* number decreases the tendency of the microdroplet to break up symmetrically;
- Mother microdroplets with larger lengths tend to break up more symmetrically, and the breakup ratio approaches 0.5;
- As the magnetic field intensity in the center of the T-junction increases, microdroplets break up more asymmetrically, and the breakup ratio tends toward 1. By increasing the magnetic field intensity at the T-junction, the likeliness of the asymmetrical breakup of the mother microdroplet increases, and higher values of the breakup ratio are achievable;
- Utilizing an asymmetrical magnetic field in the center of the T-junction causes a shift upward for the border curve between the breakup and non-breakup regions in the diagram of non-dimensional length versus *Ca*;
- A correlation has been obtained to predict the variations of the border curve of breakup and non-breakup regions due to changes in magnetic flux density.

This study focused on the effect of a permanent magnetic field on the process of ferrofluid microdroplet breakup. It would be interesting to study the effect of ferrofluid concentration, and geometry parameters, such as T-junction with asymmetric length or width, on the ferrofluid droplet splitting in future studies.

Nomenclature

A	Area (μm^2)
$\vec{B}$	Magnetic flux density (mT)
$\|\vec{B}\|$	Magnitude of Magnetic flux density (mT)
BR	Breakup ratio
Ca	Capillary number
d	Distance between magnet and center of T-junction (μm)
$\vec{f}$	Magnetic force applied on the ferrofluid droplet (N)
$\vec{H}$	Magnetic field strength (A/m)
L	The initial length of the ferrofluid droplet (μm)
L_c	Maximum length of the ferrofluid droplet during passing the center of T-junction (μm)
$\vec{M}$	Magnetization (A/m)
Q	Volumetric flow rate (ml/hr)

$\vec{u}$ Velocity (m/s)
W Width of the microchannel (400 µm)

Greeck symbols

μ Dynamic viscosity (mPa.s)
μ_0 Magnetic permeability coefficient in vacuum (N/A^2)
ρ Density (kg/m^3)
σ Surface tension between two fluids (mN/m)
χ_m Magnetic permeability

Subscripts

c Continuous-phase
d Discrete-phase
r Right side
tot Total

Funding

This research did not receive any specific grant from funding agencies in the public, commercial, or not-forprofit sectors.

Conflicts of interest

The authors declare that they have no known competing financial interests or personal relationships that could have appeared to influence the work reported in this paper.

The author is an Editorial Board Member/Editor-inChief/Associate Editor/Guest Editor for Scientia Iranica and was not involved in the editorial review or the decision to publish this article.

Authors contribution statement

Mohammad Aboutalebi: Conceptualization; Formal analysis; Investigation; Methodology; Validation; Visualization; Writing–review and editing.

Omid Adibi: Formal analysis; Investigation; Methodology; Visualization; Writing–review and editing.

Mohamad Ali Bijarchi: Conceptualization; Formal analysis; Methodology; Writing–review and editing.

Mohammad Behshad Shafii: Conceptualization; Methodology; Supervision; Writing–review and editing.

Siamak Kazemzadeh Hannani: Conceptualization; Methodology; Supervision; Writing–review and editing.

References

1. Shamloo, A., Vatankhah, P., and Bijarchi, M.A. "Numerical optimization and inverse study of a microfluidic device for blood plasma separation", *European Journal of Mechanics-B/Fluids*, **57**, pp. 31-39 (2016). https://doi.org/10.1016/j.euromechflu.2016.02.002.

2. Ahmadi, M.-A., Ahmadi, M.H., Alavi, M.F., et al. "Determination of thermal conductivity ratio of CuO/ethylene glycol nanofluid by connectionist approach", *Journal of the Taiwan Institute of Chemical Engineers*, **91**, pp. 383-395 (2018). https://doi.org/10.1016/j.jtice.2018.06.003.

3. Alhuyi Nazari, M., Ahmadi, M.H., Lorenzini, G., et al. "Modeling thermal conductivity ratio of CuO/ethylene glycol nanofluid by using artificial neural network", *Defect and Diffusion Forum*, **388**, pp. 39-43 (2018). https://doi.org/10.4028/www.scientific.net/DDF.388.39.

4. Joensson, H.N. and Andersson-Svahn, H. "Droplet microfluidics—a tool for protein engineering and analysis", *Lab on a Chip*, **11**(24), pp. 4144-4147 (2011). https://doi.org/10.1039/C1LC90102H.

5. Zhu, P. and Wang, L. "Passive and active droplet generation with microfluidics: a review", *Lab on a Chip*, **17**(1), pp. 34-75 (2017). https://doi.org/10.1039/c6lc01018k.

6. Chien, L.-H., Liao, W.-R., Ghalambaz, M., et al. "Experimental study on convective boiling flow and heat transfer in a microgap enhanced with a staggered arrangement of nucleated micro-pin-fins", *International Journal of Heat and Mass Transfer*, **144**, p. 12 (2019). https://doi.org/10.1016/j.ijheatmasstransfer.2019.118653.

7. Chen, C.-Y., Chen, C.-H., and Lo, L.-W. "Breakup and separation of micromagnetic droplets in a perpendicular field", *Journal of Magnetism and Magnetic Materials*, **310**(2), pp. 2832-2834 (2007). https://doi.org/10.1016/j.jmmm.2006.10.1064.

8. Gijs, M.A., Lacharme, F., and Lehmann, U. "Microfluidic applications of magnetic particles for biological analysis and catalysis", *Chemical Reviews*, **110**(3), pp. 1518-1563 (2009). https://doi.org/10.1021/cr9001929.

9. Ray, A., Varma, V., Jayaneel, P., et al. "On demand manipulation of ferrofluid droplets by magnetic fields", *Sensors and Actuators B: Chemical*, **242**, pp. 760-768 (2017). https://doi.org/10.1016/j.snb.2016.11.115.

10. Ganguly, R., Sen, S., and Puri, I.K. "Heat transfer augmentation using a magnetic fluid under the influence of a line dipole", *Journal of Magnetism and Magnetic Materials*, **271**(1), pp. 63-73 (2004). https://doi.org/10.1016/j.jmmm.2003.09.015.

11. Ding, Y., Howes, P.D., and deMello, A.J. "Recent advances in droplet microfluidics", *Analytical chemistry*, **92**(1), pp. 132-149 (2019). https://doi.org/10.1021/acs.analchem.9b05047.

12. Raveshi, M.R., Abdul Halim, M.S., Agnihotri, S.N., et al. "Curvature in the reproductive tract alters sperm–surface interactions", *Nature communications*, **12**(1), 3446 (2021). https://doi.org/10.1038/s41467-021-23773-x.

13. Agnihotri, S.N., Raveshi, M.R., Bhardwaj, R., et al. "Droplet breakup at the entrance to a bypass channel in a microfluidic system", *Physical Review Applied*, **11**(3), 034020 (2019). https://doi.org/10.1103/PhysRevApplied.11.034020.

14. Agnihotri, S.N., Raveshi, M.R., Bhardwaj, R., et al. "Microvalves for integrated selective droplet generation, splitting and merging on a chip", *Microfluidics Nanofluidics*, **25**(11), pp. 1-13 (2021). https://doi.org/10.1007/s10404-021-02487-y.

15. Mashaghi, S., Abbaspourrad, A., Weitz, D.A., et al. "Droplet microfluidics: A tool for biology, chemistry and nanotechnology", *TrAC Trends in Analytical Chemistry*, **82**, pp. 118-125 (2016). https://doi.org/10.1016/j.trac.2016.05.019.

16. Tae, S.-J. and Cho, K. "Effect of flow direction on two-phase flow distribution of refrigerants at a T-junction", *Journal of Mechanical Science Technology*, **20**(5), pp. 717-727 (2006). https://doi.org/10.1007/Bf02915989.

17. Jhun, C.G., Song, J.-K., and Gwag, J.S. "Highly mono-dispersed liquid crystal capsules with core–shell structure", *Physica Scripta*, **94**(5), 055001 (2019). https://doi.org/10.1088/1402-4896/ab0990.

18. Leshansky, A., and Pismen, L. "Breakup of drops in a microfluidic T junction", *Physics of Fluids*, **21**(2), p. 6 (2009). https://doi.org/10.1063/1.3078515.

19. Bedram, A. and Moosavi, A. "Numerical investigation of droplets breakup in a microfluidic T-junction", *Applied Mechanics and Materials*, **110**, pp. 3269-3277 (2012). https://doi.org/10.4028/www.scientific.net/AMM.110-116.3269.

20. Bedram, A. and Moosavi, A. "Droplet breakup in an asymmetric microfluidic T junction", *The European Physical Journal E*, **34**(8), p. 8 (2011). https://doi.org/10.1140/epje/i2011-11078-7.

21. Leshansky, A., Afkhami, S., Jullien, M.-C., et al. "Obstructed breakup of slender drops in a microfluidic T junction", *Physical Review Letters*, **108**(26), p. 5 (2012). https://doi.org/10.1103/PhysRevLett.108.264502.

22. Jullien, M.-C., Ching, M.-J.T.M., Cohen, C., et al. "Droplet breakup in microfluidic T-junctions at small capillary numbers", *Physics of Fluids*, **21**(7), p. 7 (2009). https://doi.org/10.1063/1.3170983.

23. Bedram, A., Darabi, A.E., Moosavi, A., et al. "Numerical investigation of an efficient method (T-junction with valve) for producing unequal-sized droplets in micro-and nano-fluidic systems", *Journal of Fluids Engineering*, **137**(3), p. 9 (2015). https://doi.org/10.1115/1.4028499.

24. Salkin, L., Schmit, A., Courbin, L., et al. "Passive breakups of isolated drops and one-dimensional assemblies of drops in microfluidic geometries: experiments and models", *Lab on a Chip*, **13**(15), pp. 3022-3032 (2013). https://doi.org/10.1039/c3lc00040k.

25. Jangir, P. and Jana, A.K. "CFD simulation of droplet splitting at microfluidic T-junctions in oil–water two-phase flow using conservative level set method", *Journal of the Brazilian Society of Mechanical Sciences and Engineering*, **41**(2), p. 16 (2019). https://doi.org/10.1007/s40430-019-1569-2.

26. Aboutalebi, M., Bijarchi, M.A., Shafii, M.B., et al. "Numerical investigation on splitting of ferrofluid microdroplets in T-junctions using an asymmetric magnetic field with proposed correlation", *Journal of Magnetism and Magnetic Materials*, **447**, pp. 139-149 (2018). https://doi.org/10.1016/j.jmmm.2017.09.053.

27. Samie, M., Salari, A., and Shafii, M.B. "Breakup of microdroplets in asymmetric T junctions", *Physical Review E*, **87**(5), p. 8 (2013). https://doi.org/10.1103/PhysRevE.87.053003.

28. Raveshi, M.R., Agnihotri, S.N., Sesen, M., et al. "Selective droplet splitting using single layer microfluidic valves", *Sensors and Actuators B: Chemical*, **292**, pp. 233-240 (2019). https://doi.org/10.1016/j.snb.2019.04.115.

29. Agnihotri, S.N., Raveshi, M.R., Bhardwaj, R., et al. "Microfluidic valves for selective on-chip droplet splitting at multiple sites", *Langmuir*, **36**(5), pp. 1138-1146 (2020). https://doi.org/10.1021/acs.langmuir.9b03515.

30. Wu, Y., Fu, T., Zhu, C., et al. "Bubble coalescence at a microfluidic T-junction convergence: from colliding to squeezing", *Microfluidics and Nanofluidics*, **16**(1-2), pp. 275-286 (2014). https://doi.org/10.1007/s10404-013-1211-z.

31. Nguyen, N.-T., Zhu, G., Chua, Y.-C., et al. "Magnetowetting and sliding motion of a sessile ferrofluid droplet in the presence of a permanent magnet", *Langmuir*, **26**(15), pp. 12553-12559 (2010). https://doi.org/10.1021/la101474e.

32. Li, X., Dong, Z.-Q., Yu, P., et al. "Numerical investigation of magnetic multiphase flows by the fractional-step-based multiphase lattice Boltzmann method", *Physics of Fluids*, **32**(8), p. 22 (2020). https://doi.org/10.1063/5.0020903.

33. Li, X., Yu, P., Niu, X.-D., et al. "A magnetic field coupling lattice Boltzmann model and its application on the merging process of multiple-ferrofluid-droplet system", *Applied Mathematics and Computation*, **393**, p. 24 (2021). https://doi.org/10.1016/j.amc.2020.125769.

34. Mu-Feng, C., Xiang, L., Xiao-Dong, N., et al. "Sedimentation of two non-magnetic particles in

magnetic fluid", *Acta Physica Sinica*, **66**(16), p. 10 (2017). https://doi.org/10.7498/aps.66.164703.

35. Afkhami, S., Tyler, A., Renardy, Y., et al. "Deformation of a hydrophobic ferrofluid droplet suspended in a viscous medium under uniform magnetic fields", *Journal of Fluid Mechanics*, **663**, pp. 358-384 (2010). https://doi.org/10.1017/S0022112010003551.

36. Majidi, M., Bijarchi, M.A., Arani, A.G., et al. "Magnetic field-induced control of a compound ferrofluid droplet deformation and breakup in shear flow using a hybrid lattice Boltzmann-finite difference method", *International Journal of Multiphase Flow*, **146**, 103846 (2022). https://doi.org/10.1016/j.ijmultiphaseflow.2021.103846.

37. Bijarchi, M.A., Favakeh, A., and Shafii, M.B. "The effect of a non-uniform pulse-width modulated magnetic field with different angles on the swinging ferrofluid droplet formation", *Journal of Industrial and Engineering Chemistry*, **84**, pp. 106-119 (2020). https://doi.org/10.1016/j.jiec.2019.12.026.

38. Favakeh, A., Bijarchi, M.A., and Shafii, M.B. "Ferrofluid droplet formation from a nozzle using alternating magnetic field with different magnetic coil positions", *Journal of Magnetism and Magnetic Materials*, **498**, p. 6 (2020). https://doi.org/10.1016/j.jmmm.2019.166134.

39. Bijarchi, M.A., Favakeh, A., Alborzi, S., et al. "Experimental investigation of on-demand ferrofluid droplet generation in microfluidics using a Pulse-Width Modulation magnetic field with proposed correlation", *Sensors and Actuators B: Chemical*, **329**, p. 14 (2021). https://doi.org/10.1016/j.snb.2020.129274.

40. Bijarchi, M.A., Favakeh, A., Mohammadi, K., et al. "Ferrofluid droplet breakup process and neck evolution under steady and pulse-width modulated magnetic fields", *Journal of Molecular Liquids*, **343**, 117536 (2021). https://doi.org/10.1016/j.molliq.2021.117536.

41. Bijarchi, M.A., Yaghoobi, M., Favakeh, A., et al. "On-demand ferrofluid droplet formation with non-linear magnetic permeability in the presence of high non-uniform magnetic fields", *Scientific Reports*, **12**(1), p. 10868 (2022). https://doi.org/10.1038/s41598-022-14624-w.

42. Bijarchi, M.A., Favakeh, A., Sedighi, E., et al. "Ferrofluid droplet manipulation using an adjustable alternating magnetic field", *Sensors and Actuators A: Physical*, **301**, p. 111753 (2020).

43. Youesfi, M., Sarkhosh, M.H., Bijarchi, M.A., et al. "Investigating the Response of Ferrofluid Droplets in a Uniform Rotating Magnetic Field: Towards Splitting and Merging", *2023 International Conference on Manipulation, Automation and Robotics at Small Scales (MARSS)*, pp. 1-5 (2023). https://doi.org/10.1109/MARSS58567.2023.10294170.

44. Azizian, P., Mohammadrashidi, M., Abbas Azimi, A., et al. "Magnetically driven manipulation of nonmagnetic liquid marbles: Billiards with liquid marbles", *Micromachines*, **14**(1), p. 49 (2022). https://doi.org/10.3390/mi14010049.

45. Sarkhosh, M.H., Yousefi, M., Bijarchi, M.A., et al. "Manipulation of ferrofluid marbles and droplets using repulsive force in magnetic digital microfluidics", *Sensors Actuators A: Physical*, **363**, 114733 (2023). https://doi.org/10.1016/j.sna.2023.114733.

46. Zarei Saleh Abad, M., Ebrahimi-Dehshali, M., Bijarchi, M.A., et al. "Visualization of pool boiling heat transfer of magnetic nanofluid", *Heat Transfer-Asian Research*, **48**(7), pp. 2700-2713 (2019). https://doi.org/10.1002/htj.21498.

47. Wu, Y., Fu, T., Ma, Y., et al. "Active control of ferrofluid droplet breakup dynamics in a microfluidic T-junction", *Microfluidics and Nanofluidics*, **18**(1), pp. 19-27 (2015). https://doi.org/10.1007/s10404-014-1414-y.

48. Aboutalebi, M., Shafii, M.B., and Kazemzadeh Hannani, S. "Numerical study on the ferrofluid droplet splitting in a T-junction with branches of unequal widths using asymmetric magnetic field", *Journal of Applied Computational Mechanics*, **9**(2), pp. 357-370 (2023). https://doi.org/10.22055/JACM.2021.36722.2892.

49. Bijarchi, M.A., Dizani, M., Honarmand, M., et al. "Splitting dynamics of ferrofluid droplets inside a microfluidic T-junction using a pulse-width modulated magnetic field in micro-magnetofluidics", *Soft Matter*, **17**(5), pp. 1317-1329 (2021). https://doi.org/10.1039/d0sm01764g.

50. Chen, C.-Y., Chen, C.-H., and Lee, W.-F. "Experiments on breakups of a magnetic fluid drop through a micro-orifice", *Journal of Magnetism and Magnetic Materials*, **321**(20), pp. 3520-3525 (2009). https://doi.org/10.1016/j.jmmm.2009.06.066.

51. Chang, C.-W., Cheng, Y.-T., Tsai, C.-Y., et al. "Periodic flow patterns of the magnetic fluid in microchannel", *Journal of Magnetism and Magnetic Materials*, **310**(2), pp. 2844-2846 (2007). https://doi.org/10.1016/j.jmmm.2006.11.064.

52. Basu, A.S. "Droplet morphometry and velocimetry (DMV): a video processing software for time-resolved, label-free tracking of droplet parameters", *Lab on a Chip*, **13**(10), pp. 1892-1901 (2013). https://doi.org/10.1039/c3lc50074h.

53. Bijarchi, M.A. and Shafii, M.B. "Experimental investigation on the dynamics of on-demand ferrofluid

drop formation under a pulse-width-modulated nonuniform magnetic field", *Langmuir*, **36**(26), pp. 7724-7740 (2020). https://doi.org/10.1021/acs.langmuir.0c00097.

54. Mohammadrashidi, M., Bijarchi, M.A., Shafii, M.B., et al. "Experimental and theoretical investigation on the dynamic response of ferrofluid liquid marbles to steady and pulsating magnetic fields", *Langmuir*, **39**(6), pp. 2246-2259 (2023). https://doi.org/10.1021/acs.langmuir.2c02811.

55. Mohammadrashidi, M., Azizian, P., Bijarchi, M.A., et al. "Vibration and jumping of ferrofluid marbles under an initial magnetic perturbation", *Langmuir*, **39**(27), pp. 9406-9417 (2023). https://doi.org/10.1021/acs.langmuir.3c00894.

Appendix A

In this section, the uncertainty analysis has been discussed. To obtain the result, the breakup ratio is calculated based on the following Eqs:

$$BR = \frac{A_r}{A_{tot}}, \tag{A.1}$$

where, A_r and A_{tot} are the cross-section area of the mother and right daughter microdroplets, respectively. So, the breakup ratio is a function of A_r and A_{tot} ($BR = f(A_r, A_{tot})$). By taking logarithm from both sides and taking a derivative, it can be obtained as follows:

$$ln(BR) = ln\, A_r - ln\, A_{tot}\,, \tag{A.2}$$

$$\left|\frac{d(BR)}{BR}\right| = \left|\frac{dA_r}{A_r}\right| + \left|\frac{dA_{tot}}{A_{tot}}\right|. \tag{A.3}$$

By assuming the microdroplet is a rectangle with a width equal to channel width (W) and length of L, the relative error can be calculated:

$$\left|\frac{d(BR)}{BR}\right| = \left|\frac{WdL_r}{WL_r}\right| + \left|\frac{WdL_{tot}}{WL_{tot}}\right|, \tag{A.4}$$

where L_r and L_{tot} are the right and mother droplet lengths, respectively. The error for obtaining L_r and L_{tot} by an image processing software is 1 pixel, and for Ca=0.03, $|\vec{B}|$ = 170 mT, and L/W =2.64 with L_r = 100 pixels and L_{tot} = 170 pixels, the relative error is 1.6%.

Biographies

Mohammad Aboutalebi received his PhD in Mechanical Engineering from Sharif University of Technology, Tehran, Iran, where he also earned his BSc in 2006 and MSc in 2009. Dr. Aboutalebi's research focuses on experimental tests, heat transfer, and micro and nano fluids, with a particular interest in microdroplets. His work contributes to the understanding and application of advanced fluid mechanics and heat transfer principles.

Omid Adibi is an Assistant Professor in the Energy Management Group at Niroo Research Institute, Tehran, Iran. He received his MEng in 2012 and PhD in 2018 from Sharif University of Technology, Tehran, Iran. Dr. Adibi specializes in thermal management and computational fluid dynamics, with research interests in building energy modeling, phase change materials, and optimization of engineering equipment. His work focuses on innovative approaches to energy management and reducing energy consumption.

Mohamad Ali Bijarchi is an Assistant Professor in the Department of Mechanical Engineering at Sharif University of Technology, Tehran, Iran. He received his BSc and MSc degrees in Mechanical Engineering from the University of Tehran in 2012 and 2014, respectively, and completed his PhD at Sharif University of Technology in 2020. His research interests span diverse areas, including AI applications in fluid mechanics and heat transfer, renewable energies, battery thermal management, ferrohydrodynamics, and microfluidics, with a focus on innovative approaches to energy and thermal challenges.

Mohammad Behshad Shafii is a Professor in Mechanical Engineering at Sharif University of Technology, Tehran, Iran. He earned his BEng from Sharif University of Technology in 1996 and his PhD from Michigan State University in 2005. Dr. Shafii's research focuses on thermal management and fluid dynamics, including heat pipes, fluid diagnostic techniques, and solar energy applications. His work combines theoretical and experimental approaches to advance heat transfer and fluid mechanics.

Siamak Kazemzadeh Hannani is a Professor of Mechanical Engineering at Sharif University of Technology, Tehran, Iran, and a member of the Center of Excellence in Energy Conversion. He received his PhD in Mechanical Engineering from the University of Lille, France, in 1996. Dr. Hannani's research interests focus on finite element methods, heat transfer, and turbulence modeling, contributing to advancements in computational methods for engineering applications.